

Ultrasonic Investigation of the Lambda Transition in $\text{NH}_4\text{Br}^\dagger$

Carl W. Garland and Carolyn K. Choo

Department of Chemistry and Center for Materials Science and Engineering, Massachusetts Institute of Technology, Cambridge, Massachusetts 02139

(Received 30 April 1973)

The ultrasonic-attenuation coefficient α has been measured in the disordered phase of NH_4Br at 10, 30, and 50 MHz as a function of temperature for the [100] longitudinal wave and the [110] transverse wave associated with the c' shear. By combining these data with available ultrasonic- and hypersonic-velocity data it is possible to determine the dynamical behavior near the order-disorder transition if one assumes a single-relaxation model. The critical relaxation time for the longitudinal wave is well represented by $1/\tau$ (in units of 10^8 sec^{-1}) = $1.8 + 1780\epsilon^{1.0}$, where ϵ is the reduced temperature $(T - T_\lambda)/T_\lambda$. The transverse relaxation time is quite similar. The critical attenuations themselves can be approximately represented by a power law of the form $\alpha_c = S\omega^2\epsilon^{-l}$, where $l \approx 1.35$. It was found possible to obtain an essentially single domain NH_4Br crystal in the tetragonal ordered phase by cooling the crystal slowly with a small temperature gradient along one of its axes. Longitudinal and shear velocities were measured in the ordered phase as a function of temperature from 120 °K to $T_\lambda \approx 234.5$ °K. Critical attenuation measured at 10 MHz for the longitudinal wave was well described by a power law with the exponent $l = 0.75$.

I. INTRODUCTION

Both NH_4Cl and NH_4Br crystals undergo order-disorder transitions of the λ type involving the relative orientations of the tetrahedral NH_4^+ ions. At room temperature, both crystals have a disordered CsCl-type cubic structure with the NH_4^+ ions distributed at random with respect to two equivalent orientations in the cubic cell. However, there are major differences between the types of ordering observed in the chloride and in the bromide. In the case of NH_4Cl , there is a single λ line marking the transition between the disordered cubic phase and a "parallel" ordered cubic phase. The phase diagram for NH_4Br is much more complicated,¹ and the λ transition at low pressures involves an ordered tetragonal phase with "antiparallel" chains of NH_4^+ ions. Although the λ temperatures are fortuitously similar at 1 atm ($T_\lambda \approx 242$ °K for NH_4Cl and 234.5 °K for NH_4Br), the λ lines have slopes of opposite sign. Recent theoretical works² indicate that there are two competing interactions between neighboring ammonium ions—a direct octopole-octopole interaction and an indirect interaction via the polarizable halide ion. This octopole-dipole term appears to be dominant in NH_4Br and explains the "antiferromagnetic" ordering in that case.

Thus it is of interest to compare the dynamical behavior of NH_4Br near its λ transition with the analogous behavior recently reported for NH_4Cl .³ Acoustic attenuation and dispersion measurements in NH_4Cl have been carried out at 1 atm and at high pressures, and these data have been analyzed in terms of a single-relaxation formalism to evaluate the critical variation of the relaxation time τ for long-range ordering. A similar analy-

sis will be presented here for the acoustic behavior of NH_4Br in its disordered phase at 1 atm. Unlike the case of NH_4Cl , where only longitudinal waves exhibit dispersion and critical attenuation, the c' shear wave propagating in the [110] direction and polarized perpendicular to [001] is also strongly attenuated near T_λ in NH_4Br . In addition to this qualitative difference, the critical exponents for the divergence of τ (as obtained from data on [100] longitudinal waves) are quite different in the two crystals.

Ultrasonic-velocity measurements in NH_4Br have been made previously over a wide range of temperatures and pressures.^{1,4} Thus the low-frequency limiting values of all three independent elastic constants c_{11} , c_{44} , and $c' = (c_{11} - c_{12})/2$ are well known in the disordered phase. The velocity and attenuation of hypersonic acoustic waves have been determined at room temperature as a function of frequency from Brillouin scattering measurements; in addition, the velocity of the [110] longitudinal wave has been measured as a function of temperature at ~ 16 GHz.⁵ On the basis of these data it is possible to estimate the temperature dependence of the velocity dispersion for the c_{11} and c' waves. In this paper we report the ultrasonic attenuation of c_{11} and c' waves in disordered NH_4Br as a function of temperature and frequency at 1 atm. By assuming a single-relaxation model, we are then able to determine the critical behavior of the relaxation time for $T > T_\lambda$.

Previous ultrasonic investigations of NH_4Br have been largely confined to the disordered phase. When a single crystal undergoes the transition from the cubic disordered phase to the tetragonal ordered phase, many ordered domains are formed with their tetragonal axes oriented randomly along the

original cubic axes. Such a multidomain crystal scatters sound very strongly, and the echo pattern disappears for longitudinal waves and the c' shear wave. In the present investigation, it was found possible to obtain an essentially single-domain ordered crystal. Thus we were able to measure the velocities of both longitudinal and shear waves and the anomalous attenuation of the longitudinal wave as a function of temperature in the ordered phase.

II. EXPERIMENTAL PROCEDURES

The ultrasonic techniques used in this investigation were very similar to those used previously to study ammonium chloride. Attenuation measurements were carried out with a single-transducer, pulse-echo method using Matec ultrasonic equipment.⁶ Velocity measurements were made at 10 MHz with a pulse-superposition method.⁷

A Lauda refrigerating circulator and dry-ice heat exchanger were used for measurements in the disordered phase. Liquid nitrogen and a variable-pressure transfer gas were used for measurements in the ordered phase. In both cases, regulation of the temperature of a copper sample holder was achieved with a Bayley model-250 proportional temperature controller. The resulting temperature stability, as measured with a calibrated Rosemount platinum resistance thermometer, was ± 5 m°K.

The NH_4Br single crystals used in this experiment were from the same batch as those studied in an earlier high-pressure investigation.¹ They were at least 99.9% pure, were free from visible defects, and had well-developed (100) faces which were parallel to within ± 0.0001 cm. Some preliminary measurements in the [100] direction were made using a slightly imperfect crystal with a length $L = 0.7066$ cm. Final measurements in that direction were made on a larger and more perfect crystal, denoted as crystal I. With the exception of attenuation values in the ordered phase, data obtained on these two crystals agreed well with each other. Crystal Ia was used as grown for longitudinal attenuation measurements in the disordered phase; the length of this crystal in the [100] direction was 0.8928 ± 0.0001 cm at 20°C. Subsequently, one face of this crystal was water damaged and a new face was flycut parallel to the undamaged (100) face; the new length was 0.8179 ± 0.0005 cm at 20°C. This crystal, designated as crystal Ib, was then used for measurements in the ordered phase. Crystal II was flycut to obtain a pair of (110) faces; the parallelity of these faces was within ± 0.0003 cm and the length along the [110] direction was 0.7562 cm at 20°C. It should be noted that NH_4Br crystals are soft and hygro-

scopic and must be handled with considerable care.

The transition temperature T_λ for each crystal was determined by measuring the shear velocity corresponding to the elastic constant c_{44} . This shear wave is not attenuated near T_λ and can even be propagated in a polydomain ordered crystal. Furthermore, this shear velocity undergoes a very rapid variation at the transition. Indeed, the temperature coefficient $(\partial c_{44}/\partial T)_p$ changes abruptly from a small negative value in the disordered phase to a very large positive value, and the transition point is easily established. The λ temperature was found to be (234.3 ± 0.1) °K in crystal I and (234.8 ± 0.1) °K in crystal II. These values agree reasonably with the value 234.5°K cited by Garland and Yarnell.⁴

Dow resin 276-V9 was used to bond the $\frac{1}{4}$ -in.-diam quartz transducers to the NH_4Br crystals. However, this bond broke when the sample was cooled below 160°K, and the less viscous Dow-Corning 200 silicone fluids were used for measurements in the ordered phase.

It was found possible to obtain an effectively "single-domain" NH_4Br crystal in the tetragonal ordered phase by cooling the crystal slowly through the transition after a temperature gradient has been established along one of the [100] axes. This gradient was obtained by placing a small heating element in good thermal contact with the face opposite from the transducer (which is itself in good thermal contact with the copper sample holder). The optimal gradient, as measured with a gold-chromel difference thermocouple, was 4 to 5°K cm⁻¹. The gradient heater was turned on and the sample holder was maintained at ~ 237 °K for several hours to allow the system to achieve a steady-state temperature distribution. The sample holder was then cooled slowly to about 210°K. The rate of cooling was not crucial, but a constant rate of 4°K h⁻¹ seemed to give the best results. The criterion for deciding whether a single domain had been formed was the ability to propagate longitudinal waves and obtain a good exponential echo pattern with at least five echoes at ~ 200 °K. Ultrasonic pulses were not propagated in the sample during the cooling process, and the gradient heater was turned off before the echo pattern was inspected. Although there is no direct evidence about the tetragonal domain structure formed below T_λ , the observed ultrasonic behavior is consistent with a single dominant domain and we shall consider the ordered tetragonal phase to be a single-domain crystal. After the gradient is turned off, there is no indication of any change in the domain structure with time or with temperature variations (as long as the temperature is kept below T_λ).

III. RESULTS

A. Attenuation in the Disordered Cubic Phase

Longitudinal waves. The attenuation α of longitudinal waves propagating in the [100] direction (c_{11} wave) has been measured as a function of temperature at 10, 30, and 50 MHz. Plots of the observed α values versus f^2 at various constant temperatures between 236 and 255 °K gave a family of straight lines with a common intercept $\alpha_0 = 0.3 \pm 0.1$ dB cm⁻¹. Thus the total attenuation consists of a large critical attenuation α_c related to the order-disorder transition and a small background attenuation α_0 which is independent of frequency and temperature. This background attenuation is caused by various effects such as beam spreading due to the finite size of the transducer, scattering from imperfections in the sample, and energy losses in the bond between the transducer and the sample.

The behavior of the critical attenuation $\alpha_c = \alpha_{\text{obs}} - \alpha_0$ is shown in Fig. 1, where $\log \alpha_c$ is plotted against $\log(T - T_\lambda)$. The straight lines shown in this figure represent the best fit to the data with a power-law of the form

$$\alpha_c (\text{Np cm}^{-1}) = S \omega^2 \epsilon^{-l}, \quad (1)$$

where $\omega = 2\pi f$ and ϵ is the reduced temperature $|T - T_\lambda|/T_\lambda$. The values of the parameters are $S = (1.4 \pm 0.3) \times 10^{-19}$ sec² cm⁻¹ and $l = 1.35 \pm 0.05$. In fact, the data show a definite systematic deviation from a simple power law. Smooth-curve values of α_c/ω^2 as obtained from the slopes of α_{obs} -vs- f^2 plots are given in Table I and will be used in further analysis of these data.

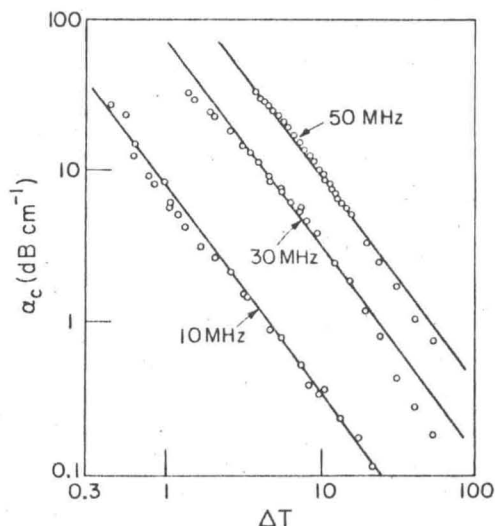


FIG. 1. Log-log plots of α_c vs ΔT (in °K) for [100] longitudinal waves in the disordered cubic phase of NH_4Br . The lines represent a simple power-law fit to the data using Eq. (1).

TABLE I. Smooth-curve values of α_c/ω^2 (in units of 10^{-18} Np sec² cm⁻¹) at different values of $\Delta T = T - T_\lambda$.

| c_{11} wave | | c' wave | | c_{long} wave | |
|-----------------|---------------------|-----------------|---------------------|------------------------|---------------------|
| ΔT (°K) | α_c/ω^2 | ΔT (°K) | α_c/ω^2 | ΔT (°K) | α_c/ω^2 |
| 1.5 | 96.5 | 0.8 | 77.4 | -1.57 | 530 |
| 2.0 | 74.3 | 1.0 | 65.2 | -1.89 | 471 |
| 2.5 | 60.2 | 1.2 | 59.8 | -2.44 | 389 |
| 3.0 | 48.5 | 1.5 | 47.2 | -3.06 | 332 |
| 3.5 | 40.9 | 1.8 | 40.4 | -4.21 | 238 |
| 4.0 | 35.6 | 2.0 | 35.7 | -5.99 | 191 |
| 4.5 | 30.8 | 2.5 | 28.3 | -7.45 | 170 |
| 5.5 | 24.6 | 3.0 | 23.2 | -9.46 | 145 |
| 6.5 | 20.2 | 3.5 | 18.4 | -11.27 | 133 |
| 7.5 | 16.7 | 4.0 | 14.6 | -12.84 | 117 |
| 8.5 | 14.0 | 4.5 | 12.3 | -15.09 | 99 |
| 10.5 | 10.3 | 5.0 | 10.5 | -17.74 | 92 |
| 12.5 | 7.82 | 5.5 | 9.34 | -20.18 | 79 |
| 13.5 | 6.90 | 6.0 | 8.09 | -22.98 | 67 |
| 15.5 | 5.64 | 6.5 | 7.21 | -24.98 | 66 |
| 17.5 | 4.65 | 7.0 | 6.42 | -28.15 | 59 |
| 20.5 | 3.60 | 7.5 | 5.84 | -32.51 | 51 |
| | | 8.0 | 5.28 | -36.56 | 50 |
| | | 9.0 | 4.23 | -42.07 | 46 |
| | | 10.0 | 3.50 | -52.21 | 40 |
| | | 12.0 | 2.63 | -63.29 | 36 |

The most important factor limiting the accuracy of the attenuation is a slight nonexponential character in the echo pattern. The average deviation in the α_{obs} values obtained from adjacent pairs of echoes was $\sim 10\%$ in regions of small or moderate attenuation. Since the character of the echo pattern remained essentially the same throughout a run, changes in α_{obs} with temperature could be determined with somewhat higher accuracy. The scatter in the data indicates that 5% would be a reasonable estimate of the random error.

The attenuation of longitudinal waves propagating in the [110] direction was measured only at 10 MHz since good echo patterns could not be obtained at higher frequencies. The (110) faces of crystal II had deteriorated during an extensive set of earlier measurements on the c' shear wave, and recutting this crystal did not improve the parallelity of the faces or reduce the distortion in the high-frequency echo pattern. The critical attenuation for this wave could be shown to agree with that for the c_{11} wave at 10 MHz if the background attenuation α_0 was assumed to have the rather large value of 1.8 dB cm⁻¹ in the [110] direction. However, these limited data did not permit us to make any conclusive determination of the dependence of α_c/ω^2 on the direction of propagation of longitudinal waves in NH_4Br . Attenuation measurements on NH_4Cl have shown that α_c values in the disordered phase of that crystal are essentially the same for longitudinal waves propagating in the [100] and [110] directions,⁸

and it is likely that the values in these two directions are very similar, if not identical, in NH_4Br also.

Transverse waves. There is no appreciable attenuation for ultrasonic shear waves corresponding to the elastic constant c_{44} . However, the transverse wave propagating in the $[110]$ direction and polarized perpendicular to the $[001]$ direction (c' wave) does exhibit critical attenuation. Initially it was difficult to obtain a satisfactory echo pattern at high frequencies, but proper impedance matching and improvement of the parallelism of the (110) faces by repeated flycutting of crystal II resulted in a reasonably good exponential pattern of more than 15 echoes at room temperature. Because the attenuation of this c' wave was smaller than that of the c_{11} wave, it was possible to carry out 30 and 50 MHz measurements closer to T_λ than before. Plots of α vs f^2 were linear at all temperatures, but the intercept was not independent of temperature as in the case of the c_{11} wave. The background attenuation α_0 had an essentially constant value of 1.3 dB cm^{-1} in the range $4.5 < \Delta T < 12.5^\circ\text{K}$ but increased steadily on approaching the transition (for example, $\alpha_0 = 2.1$ at $\Delta T = 2.37^\circ\text{K}$ and 4.8 at $\Delta T = 0.80^\circ\text{K}$). Smooth-curve values of α_c/ω^2 as obtained from the slopes of these α_{obs} -vs- f^2 plots are given in Table I. It is possible to approximate these transverse α_c/ω^2 values with the power law given in Eq. (1), but since a log-log plot of α_c/ω^2 vs ϵ shows distinct curvature, one is not able to determine an unambiguous value for the exponent l . Values of l between 1.35 and 1.5 are compatible with the data: for $l = 1.35$, one finds $S = 0.6 \times 10^{-19} \text{ sec}^2 \text{ cm}^{-1}$; for $l = 1.5$, the corresponding $S = 0.3 \times 10^{-19} \text{ sec}^2 \text{ cm}^{-1}$.

B. Attenuation in the Tetragonal Ordered Phase

Since no measurements were made below T_λ on crystal II, we observed only the longitudinal attenuation corresponding to that measured for the c_{11} wave in the disordered phase. It is not known for certain that the ordered crystal consisted of a single domain. Even if it did, the tetragonal axis could have been oriented either parallel or perpendicular to the direction of sound propagation (see Sec. III C). Since the longitudinal attenuation and velocity measurements were made in the same run, without heating the crystal above T_λ , the α values reported here and the $c_{1\text{on}z}$ values reported in Sec. III C definitely correspond to the same configuration of the ordered crystal.

The longitudinal attenuation in the tetragonal phase was only measured at 10 MHz since echoes could not be obtained at higher frequencies between 200°K and the transition. The data reported here were obtained from an echo pattern which was as

exponential as those in the disordered phase. Far from the transition, five echoes were measured and the average deviation of the attenuation values obtained from different echo pairs was less than 10%. (Two preliminary runs on the somewhat imperfect crystal with path length $2L = 1.4132 \text{ cm}$ gave much larger α values and more scatter in the data as a function of temperature. This suggests the necessity of having a very good single crystal in order to achieve a single domain in the tetragonal phase.)

A simple power-law dependence of $\alpha_c = \alpha_{\text{obs}} - \alpha_0$ on ΔT could be obtained when α_0 was assigned any constant value between 0.3 and 0.7 dB cm^{-1} . In view of the fact that α_0 was 0.3 dB cm^{-1} in the disordered phase, a value of 0.5 dB cm^{-1} was assumed to be a reasonable choice for the ordered phase since some additional background attenuation would be expected owing to imperfections in the domain structure. The α_c values shown in Fig. 2 and the α_c/ω^2 values given in Table I were calculated using this choice of α_0 . As indicated by Fig. 2, the 10-MHz longitudinal attenuation can be well represented by Eq. (1) with $S = (130 \pm 30) \times 10^{-19} \text{ sec}^2 \text{ cm}^{-1}$ and $l = 0.75 \pm 0.05$.

C. Velocity Measurements

The ultrasonic velocity u in the tetragonal ordered phase has been measured at 10 MHz by bonding a transducer to one of the (100) faces of a disordered cubic crystal and cooling the crystal slowly with a temperature gradient applied parallel to the direction of sound propagation (see Sec. II). When a good echo pattern was observed be-

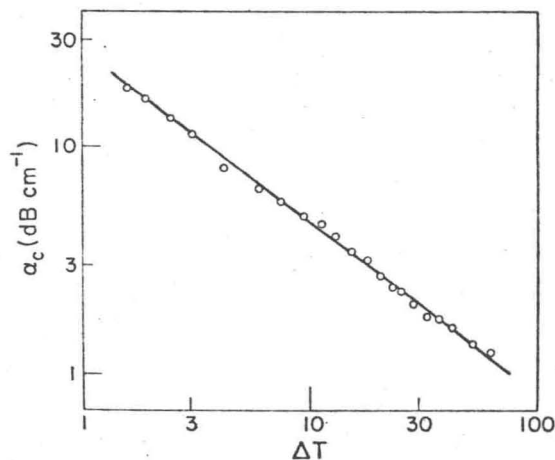


FIG. 2. Log-log plot of α_c vs ΔT (in $^\circ\text{K}$) for a 10 MHz longitudinal wave in the tetragonal ordered phase of NH_4Br . These α_c values were obtained using $\alpha_0 = 0.5 \text{ dB cm}^{-1}$. The line represents a power-law fit to the data using Eq. (1).

low T_λ for longitudinal waves, it was assumed that the crystal consisted of a single tetragonal domain. However, there could have been multidomain regions near the surface or a few large domains with their tetragonal axes perpendicular to each other. The velocity measurements cited below strongly support the view that the crystal was effectively a single domain along the acoustic path, but the data are not definitive. Even if the crystal does become a single domain, the orientation of the tetragonal axis is not known and could be different each time the crystal is cooled below T_λ .⁹ Depending on the orientation of the tetragonal axis, different thermal-expansion correction factors are needed to calculate the elastic stiffness $c = \rho u^2$ as a function of temperature. There are two possible cases: (a) The tetragonal axis is parallel to the direction of propagation of the sound wave:

$$\rho u^2 = \frac{\rho^0 (2L^0)^2}{\delta^2} \frac{(a_1^0/a_1)^2}{(a_3^0/a_3)} \quad (2)$$

(b) The tetragonal axis is perpendicular to the direction of propagation of the sound wave:

$$\rho u^2 = \frac{\rho^0 (2L^0)^2}{\delta^2} \frac{a_3^0}{a_3} \quad (3)$$

In Eqs. (2) and (3), δ is the round-trip transit time for the acoustic pulse, ρ is the mass density, $2L$ is the round-trip path length in the crystal, a_1 is the lattice parameter of one of the two equivalent axes, and a_3 is that of the tetragonal axis. The superscript zero denotes the values at a convenient reference temperature, which is 20 °C. The values $\rho^0 = 2.4336 \text{ g cm}^{-3}$ and $a_1^0 = a_3^0 = 4.0580 \text{ \AA}$ were taken from Garland and Yarnell.⁴ The values of a_1 and a_3 as functions of temperature were taken from Bonilla, Garland, and Schumaker,¹⁰ since their values fall between those obtained in two independent measurements by Hovi and co-workers.¹¹

The elastic constants obtained from shear-wave measurements are shown in Fig. 3, and those obtained from longitudinal waves in Fig. 4. Smooth-curve values are given in Table II. In the case of shear waves, two independent sets of measurements on the same crystal were carried out under exactly the same conditions except that the Y -cut quartz transducer (and thus the direction of polarization) was rotated by 90°. The elastic constants calculated from these two sets of data were in excellent agreement if it were assumed that the tetragonal axis was parallel to the propagation direction for the first run and perpendicular to it for the second run. If either Eq. (2) or (3) were used for both sets of data, the resulting ρu^2 values showed a systematic difference of about 0.8%. Thus the shear elastic constant measured in this experiment is almost certainly c_{44} . As can

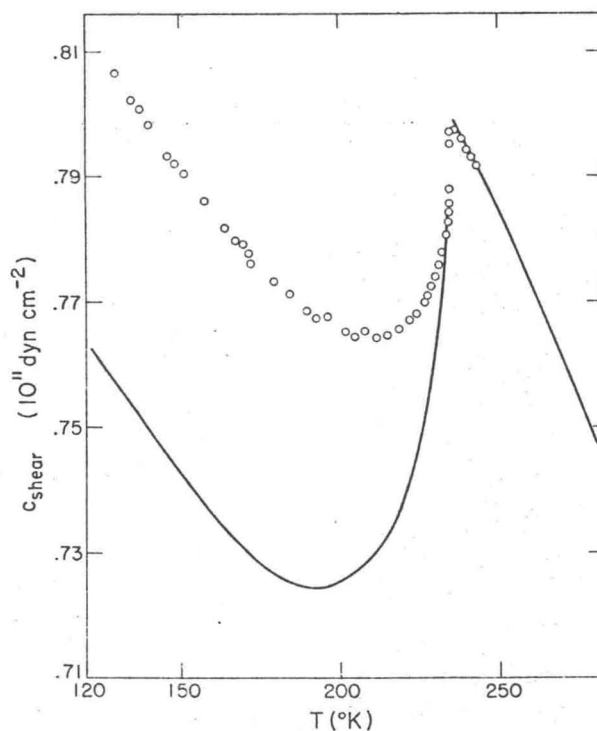


FIG. 3. Temperature dependence of c_{shear} as determined from a "single-domain" crystal in the tetragonal ordered phase. It is probable, but not certain, that these data represent c_{44} values in the ordered phase (see text). The solid line represents the well-characterized variation of c_{44} in the disordered cubic phase above T_λ and the average shear stiffness \bar{c} reported previously from measurements on multidomain ordered crystals (Ref. 4).

be seen from Fig. 3, the variation of c_{shear} is very rapid just below T_λ . Indeed, the value changes from 0.783 at 234 °K to 0.797 at 234.5 °K. It is possible that there is a discontinuous jump in the shear stiffness and hysteresis in the transition temperature, as is seen in NH_4Cl at 1 atm.⁷ However, such effects must be very small if they do occur. We estimate that $\Delta c = 0.032 \times 10^{11} \text{ dyn cm}^{-2}$ and $\Delta T = 40 \text{ m}^\circ\text{K}$ are upper limits on the possible discontinuity and hysteresis.

In the case of longitudinal waves, measurements were made on two different crystals but the orientations must have been fortuitously the same since the ρu^2 values agree on using either Eq. (2) or (3). Thus we do not know which longitudinal elastic constant has been measured in this experiment. It was arbitrarily assumed that the tetragonal axis was parallel to the propagation direction,⁹ and Eq. (2) was used in calculating the c_{long} values in Fig. 4 and Table II. If Eq. (3) had been used instead, the resulting values of c_{long} would all be lower by roughly 0.8%.

The scatter in the data indicates that the random errors in the elastic constants are about 0.1%.

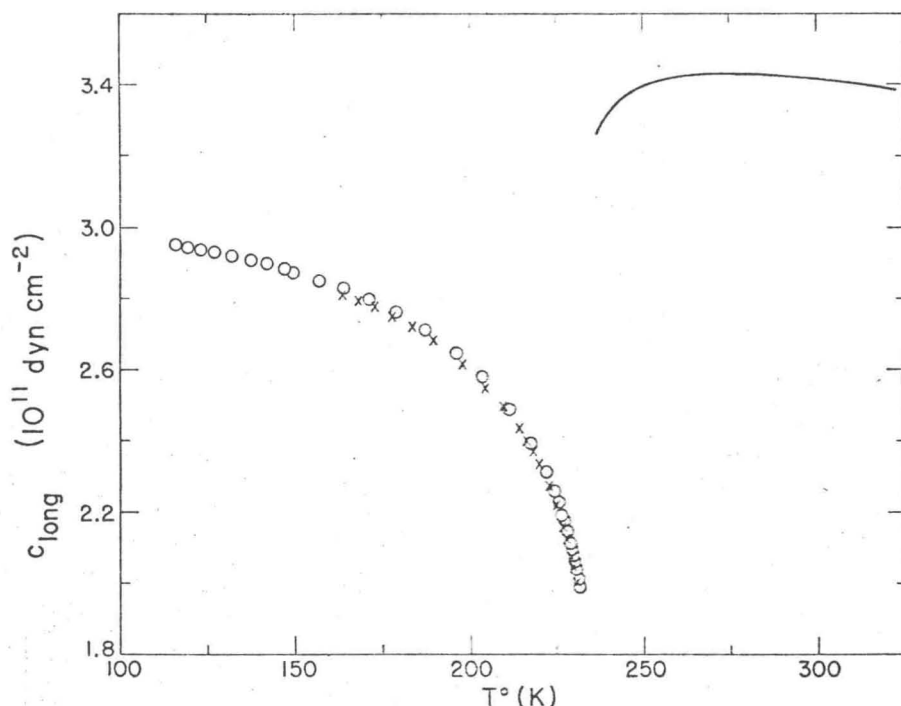


FIG. 4. Temperature dependence of c_{long} as determined from a single-domain crystal in the tetragonal ordered phase. The solid line shows the smooth-curve variation of c_{11} in the disordered phase (Ref. 4). The circles indicate data obtained on crystal Ib, and the crosses denote data obtained on the crystal with path length $2L = 1.4132$ cm.

Possible systematic errors arise not only from the ambiguity in the orientation of the tetragonal axis but also from the choice of the $n = 0$ condition⁷ for the pulse-superposition method. For shear waves, where the echo pattern could be followed through the transition region, the choice of $n = 0$ was made by matching the present c_{44} values above T_λ with those reported previously.⁴ For longitudinal waves, it was necessary to establish the choice of $n = 0$ independently in the ordered phase. As a check on this choice, c_{long} was measured on two crystals of different lengths, and Fig. 4 shows that the results are in good agreement.

IV. DISCUSSION

There are no elastic constant data in the tetragonal phase with which to compare our present results except for the average shear stiffness \bar{c} obtained from measurements on multidomain crystals.⁴ As shown in Fig. 3, the temperature variation of \bar{c} is qualitatively similar but quantitatively very different than the c_{shear} variation determined in a single-domain crystal. It was thought previously that \bar{c} represented the average $(2c_{44} + c_{66})/3$, which would result from a random orientation of the tetragonal axes of the domains along the directions of the three equivalent axes of the disordered cubic crystal. This now seems questionable. If the assignment of c_{shear} as c_{44} is correct, then c_{66} would have rather low values (a minimum value of 0.637×10^{11} dyn cm⁻² at $\sim 190^\circ\text{K}$ and 0.658×10^{11} at 130°K). Such a large tetragonal

"splitting" between c_{44} and c_{66} seems unlikely. Another possible explanation for the low \bar{c} values could be that the effective acoustic pathlength is larger in the multidomain crystal owing to reflections of the wave at domain boundaries. It should also be noted that the minimum in c_{shear} occurs at $\sim 210^\circ\text{K}$, whereas the minimum in \bar{c} is at $\sim 190^\circ\text{K}$. A minimum value near 210°K is more reasonable in view of the lattice-parameter variation.¹⁰ It is known that the shear stiffness c_{44} is a sensitive function of volume in the case of NH_4Cl .¹² By analogy, the rapid decrease in c_{shear} for NH_4Br

TABLE II. Smooth-curve values of the elastic constants c_{long} and c_{shear} (in units of 10^{11} dyn cm⁻²) for a single-domain crystal of NH_4Br in the tetragonal phase. The number of significant figures does not indicate the absolute accuracy.

| T ($^\circ\text{K}$) | c_{long} | c_{shear} | T ($^\circ\text{K}$) | c_{long} | c_{shear} |
|--------------------------|-------------------|--------------------|--------------------------|-------------------|--------------------|
| 120 | 2.941 | ... | 200 | 2.605 | 0.7654 |
| 130 | 2.920 | 0.8056 | 205 | 2.555 | 0.7648 |
| 140 | 2.898 | 0.7981 | 210 | 2.498 | 0.7643 |
| 150 | 2.870 | 0.7910 | 215 | 2.429 | 0.7645 |
| 155 | 2.854 | 0.7876 | 220 | 2.342 | 0.7660 |
| 160 | 2.838 | 0.7842 | 225 | 2.225 | 0.7689 |
| 165 | 2.813 | 0.7810 | 229 | 2.092 | 0.7730 |
| 170 | 2.790 | 0.7779 | 230 | 2.048 | 0.7742 |
| 175 | 2.767 | 0.7751 | 231 | 1.998 | 0.7758 |
| 180 | 2.745 | 0.7726 | 231.5 | 1.980 | 0.7768 |
| 185 | 2.718 | 0.7703 | 232 | ... | 0.7775 |
| 190 | 2.685 | 0.7683 | 233 | ... | 0.7796 |
| 195 | 2.648 | 0.7665 | 234 | ... | 0.7825 |

just below T_λ would be expected because of the anomalous expansion which takes place on ordering. The fact that NH_4Br expands on cooling into the tetragonal ordered phase whereas NH_4Cl undergoes an anomalous contraction on transforming into its cubic ordered phase presumably explains the observation that $c_{1\text{ong}}$ far below T_λ is smaller than c_{11} in the disordered phase for NH_4Br (see Fig. 4), while the opposite is true for NH_4Cl .⁷

Our attenuation data can be compared with the recently reported results of Velichkina and co-workers,¹³ who measured the [100] longitudinal attenuation at 5, 15, and 25 MHz in the range $5 \geq T - T_\lambda \geq -6$ °K. Their method involves measuring the relative change with temperature in the height of a single pulse transmitted through a thin crystal. This is advantageous when the attenuation is very high but not too accurate in regions of low to moderate attenuation. (Indeed, a systematic correction of ~ 4.5 dB cm^{-1} must be made to all their data owing to an unfortunate choice of the reference point from which changes in attenuation were measured.) The values of α_c/ω^2 estimated from their data are larger than those given in Table I by a roughly constant factor of about 1.5. The reason for such a multiplicative difference is unclear. It should be pointed out that their attenuation data in the multidomain ordered phase appear, rather surprisingly, to be more reliable than those in the disordered phase; α_c varies with frequency in a somewhat erratic way above T_λ but shows a good quadratic dependence below. Incidentally, the presence of multiple domains in a crystal cooled below T_λ in the absence of a thermal gradient was demonstrated by the depolarization of linearly polarized light.¹³

Velichkina *et al.* have interpreted their ordered-phase attenuation in terms of the Landau-Khalatnikov model involving a critical relaxation time $\tau = 2.2 \times 10^{-9} / (T_\lambda - T)$. This does not seem compatible with the quadratic frequency dependence of their data or with the fact that both their α_c/ω^2 values and the values in Table I vary like $(\Delta T)^{-0.75}$. If one ignores the multiplicative factor of ~ 1.5 between our results and theirs and considers only the ratio of α_c in the ordered phase to that in the disordered phase, the critical attenuation in the tetragonal ordered phase would not seem to depend on the domain structure. Yet our experience indicates that two crystals which show the same attenuation in the disordered phase can give quite different α_c values in the ordered phase, depending on the perfection of the crystal and the manner of cooling. Thus the interpretation of α_c in the ordered phase is puzzling.

Although the critical attenuation in the disordered phase can be approximately fit by a simple power law (see Fig. 1), the χ^2 value is rather large (5.9)

and the data show systematic deviations from Eq. (1). These deviations are seen to become even larger for the 25-MHz data of Velichkina *et al.* when $\Delta T < 1$ °K. Thus it is of interest to analyze the data in terms of a relaxation model. Whether a single-relaxation model is adequate to describe the low-frequency dynamical behavior of the order-disorder transition in NH_4Br is unclear. According to theoretical predictions for magnetic¹⁴ and fluid¹⁵ systems, a spectrum of relaxation times would be expected. However, none of the current theories seem to be directly pertinent to the analysis of NH_4Br . Moreover, the extensive hypersonic attenuation and dispersion data at room temperature show that, at least for temperatures far from T_λ , NH_4Br is well described by a single-relaxation model. In any event, the assumption of such a model leads to an empirical analysis of the ultrasonic attenuation data in which attractively simple behavior of both the relaxation strength and the relaxation time is obtained.

Since the critical attenuation data exhibit an f^2 frequency dependence, we shall adopt the low-frequency form of the single-relaxation expression:

$$\alpha_c = C \omega^2 \tau_{s,x}, \quad (4)$$

where α_c is the amplitude attenuation (in Np cm^{-1}), $\tau_{s,x}$ is the adiabatic relaxation time at constant strain, and the appropriate relaxation strength C is defined by

$$C = \frac{u^2(\infty) - u^2(0)}{2u(\omega)u^2(0)} \approx \frac{c^\infty - c^0}{2u(0)c^0}. \quad (5)$$

The analysis is based on using hypersonic-velocity data to estimate the high-frequency limiting stiffness c^∞ and ultrasonic data for the low-frequency limiting values $u(0)$ and $c^0 = \rho u^2(0)$. The resulting value of C at a given temperature is then combined with the corresponding experimental value of α_c/ω^2 to yield $\tau_{s,x}$. One could, of course, also analyze the data in terms of the adiabatic relaxation time at constant stress $\tau_{s,x}$. However, these two times are simply related to each other by $\tau_{s,x}/\tau_{s,x} = c^\infty/c^0$, and the behavior of $\tau_{s,x}$ does not differ in any significant way from that of $\tau_{s,x}$.

The temperature variations of c_{11}^0 and c'^0 are well known from ultrasonic measurements at 20 MHz.⁴ Values of c_{11}^∞ and c'^∞ are known at 24 °C from an analysis of Brillouin scattering data at angles corresponding to frequencies between 6.5 and 24 GHz.⁵ In order to estimate c'^∞ values near the transition, we have assumed a linear temperature dependence with a slope equal to the value of $d(c'^0)/dT$ at room temperature (see Fig. 5). This is a plausible but essentially arbitrary assumption. Fortunately, c_{11}^∞ near the transition can be estimated with much greater certainty. The hypersonic velocity of the [110] longitudinal wave is known as

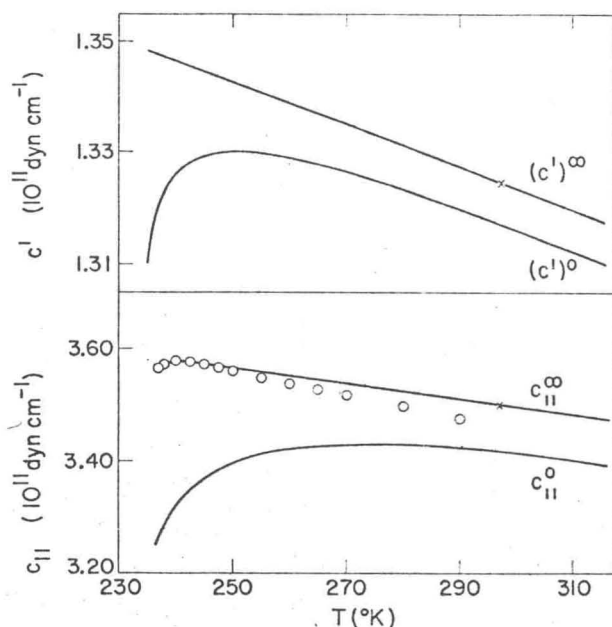


FIG. 5. Variation of the limiting values of c_{11} and c' . The smooth curves for c_{11}^0 and c'^0 are taken from Ref. 4. The crosses are infinite-frequency elastic constants reported in Ref. 5; see text for a discussion of the choice of the $c_{11}^∞$ and $c'^∞$ smooth curves. Note that the vertical scale for c' is 10 times larger than that for c_{11} .

a function of temperature at ~ 16 GHz,⁵ and the elastic stiffness corresponding to this wave is $c_L = c_{11} - c' + c_{44}$. The open circles shown in Fig. 5 represent c_{11} values calculated from $c_{11} = c_L(16 \text{ GHz}) + c'^∞ - c_{44}$. (Since there is no dis-

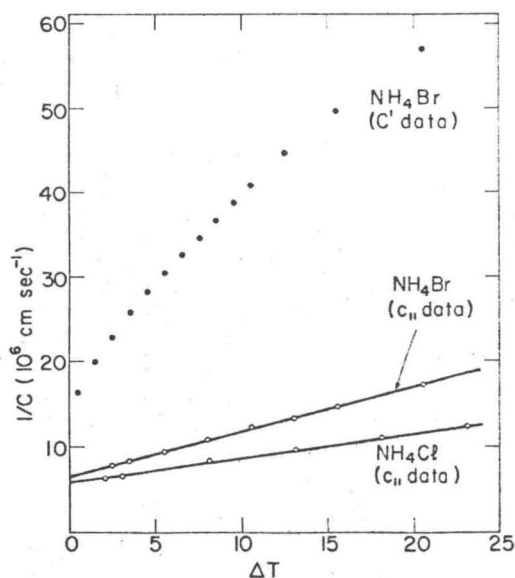


FIG. 6. Inverse relaxation strengths as a function of $\Delta T = T - T_\lambda$ (in $^\circ\text{K}$). The results for NH_4Cl are taken from Ref. 3.

persion for the [100] shear wave, $c_{44}^∞$ can be replaced by the known c_{44}^0 .) Near the transition these c_{11} values should correspond to $c_{11}^∞$ since the relaxation times becomes very long. The $c_{11}^∞$ values between 242.5 and 297 $^\circ\text{K}$ were obtained by linear interpolation (see Fig. 5). Uncertainties in $c_{11}^∞$ due to ambiguities in the $c'^∞$ values are less than 1%, which would correspond to less than a 10% possible systematic error in the relaxation strength for the c_{11} wave.

The values of the relaxation strength C calculated at various temperatures from the smooth-curve values of $c'^∞$ and c^0 are shown in Fig. 6, where $1/C$ is plotted versus $\Delta T = T - T_\lambda$. The relaxation strength for the c_{11} wave in NH_4Cl at 1 atm is also shown for comparison. This empirical plot indicates that $1/C$ varies linearly with ΔT for the [100] longitudinal wave in both NH_4Cl and NH_4Br . Indeed, this linear variation extends out to $\Delta T = 50$ for NH_4Cl .³ The inverse relaxation strength for the longitudinal wave can be represented in the form

$$C^{-1}(\epsilon) = C^{-1}(0) + b\epsilon^m, \quad (6)$$

where ϵ is the reduced temperature and m is an empirical exponent equal to 1 at 1 atm. The parameters $C^{-1}(0)$ and b are, respectively, 6.4 and 120 (in units of 10^6 cm sec^{-1}) for NH_4Br ; the

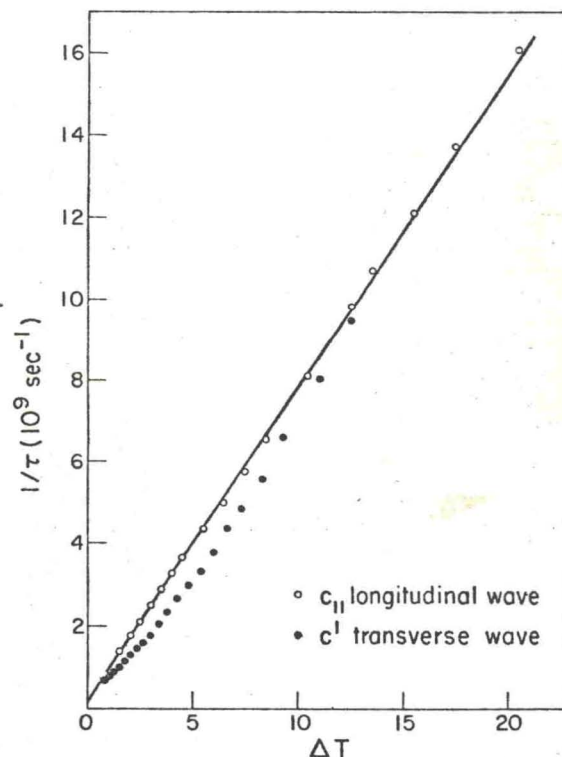


FIG. 7. Inverse relaxation times for the [100] longitudinal wave and the [110] transverse wave as a function of ΔT (in $^\circ\text{K}$).

corresponding values are 5.8 and 67.7 for NH_4Cl .³ In the case of the c' wave, the relaxation strength is less well established and it does not seem justifiable to attempt an analytical representation.

The relaxation times obtained from Eq. (4) by using the experimental α_c/ω^2 data in Table I and the above choices of C values are shown in Fig. 7, where $1/\tau$ is plotted versus ΔT . This figure indicates that the longitudinal relaxation times can be well represented by

$$1/\tau = 1/\tau(0) + a\epsilon^n, \quad (7)$$

where the subscript S, x has been dropped for convenience. The parameters $1/\tau(0)$ and a corresponding to the line in Fig. 7 are 1.8 and 1780 (in units of 10^8 sec^{-1}) and the exponent $n=1$. However, the limiting value of τ at T_λ should not be considered as well established, since a reasonably good fit can also be achieved with $1/\tau(0)=0$ and $a=1830$. The transverse relaxation times are quite similar in magnitude to the longitudinal τ values but appear to vary in a systematically different manner. Indeed, the best fit to these $1/\tau$ values gives an exponent $n=1.25$. A decision as to whether such differences are real or not will require reliable values of c'' as a function of temperature.

It is important to note that the fit to the attenuation using Eq. (4) with experimental C values and the form for τ given in Eq. (7) is much better throughout the entire temperature range than the fit with Eq. (1). The χ^2 value is quite good (0.9) and there are no systematic deviations. Even if a single relaxation formalism is not valid, the analysis we have carried out for low-frequency attenuation data is an appropriate way to treat the slowly varying strength C and obtain the exponent n for the critical relaxation frequency. That is, we can reinterpret Eq. (4) as the low-frequency form of a more general relaxation theory involving a spectrum of relaxation times. If the sound wave is coupled to the order-parameter fluctuations via a dependence of the NH_4^+ -ion interactions on the lattice parameter (volume magnetostrictive coupling in the analogous magnetic case), the major contributions to α at small ω should come from fluctuations with $k \approx \kappa$, where κ is the inverse correlation length.¹⁴ In this case, our $1/\tau \propto \Omega_\kappa$,

which is the characteristic frequency for order-parameter fluctuations with wave vector κ . Since the ammonium halides are formally quite similar to magnetic systems in their ordering, we will briefly state a few theoretical results for antiferromagnets. For an isotropic Heisenberg antiferromagnet¹⁶ n would equal $\theta\nu$, where $\theta = \frac{2}{3}$ and ν is the exponent for the inverse correlation length ($\kappa = \kappa_0\epsilon^\nu$). Thus, the conventional choice of $\nu = \frac{2}{3}$ would be consistent with our value of $n=1$. However, the Hamiltonian for NH_4Br is complicated owing to the presence of two competing interactions,² and it does not seem that one should expect agreement with theories based on an isotropic Heisenberg model. The behavior of the critical spin relaxation rate for an anisotropic Heisenberg antiferromagnetic seems to be best described by "conventional" (van Hove-type) theory,^{17,18} according to which $1/\tau$ should vary like the inverse susceptibility. Thus the exponent n should equal γ , which on the basis of scaling relations is given by $\gamma = (2-\eta)\nu$. The usual choice of $\eta=0$ and $\nu \approx \frac{2}{3}$ gives $\gamma \approx \frac{4}{3}$, in poor agreement with n . In much previous acoustic work, the variation of the relaxation strength was unknown and ignored, which led to the assumption that the exponent l in Eq. (1) was the same as n . In this view, the value $l=1.35$ would appear to be consistent with $\gamma \approx \frac{4}{3}$, but we consider this to be a fortuitous agreement. Indeed, if the conventional magnetic theory is appropriate to NH_4Br , the value of n would be consistent with the classical (Landau) exponents $\eta=0$, $\nu = \frac{1}{2}$, $\gamma=1$. Further progress requires a better understanding of the effective Hamiltonian for NH_4Br and greater development of the dynamical theories of critical phenomena.

As a final point, let us compare the dynamical aspects of the acoustic behavior of NH_4Br with those of NH_4Cl . Although the behavior of the maximum dispersion (i.e., the longitudinal relaxation strength C) is very similar in the disordered phase of NH_4Cl and NH_4Br , the variation in the relaxation time is strikingly different. For NH_4Cl at 1 atm $1/\tau = 414 \times 10^8 \epsilon^{0.6} \text{ sec}^{-1}$ up to $\Delta T = +50^\circ\text{K}$.³ Furthermore, there is no dispersion or critical attenuation associated with the c' wave in NH_4Cl . Thus the dynamical critical behavior in these two isomorphous crystals differs considerably.

¹Work supported in part by the National Science Foundation.

²C. W. Garland and R. A. Young, *J. Chem. Phys.* **49**, 5282 (1968).

³Y. Yamada, M. Mori, and Y. Noda, *J. Phys. Soc. Jap.* **32**, 1565 (1972); A. Hüller, *Z. Phys.* **254**, 456 (1972).

⁴C. W. Garland and R. J. Pollina, *J. Chem. Phys.* **58**, 5002 (1973).

⁵C. W. Garland and C. F. Yarnell, *J. Chem. Phys.* **44**, 1112 (1966).

⁶G. J. Rosasco, C. Benoit, and A. Weber, in *Proceedings of the Second International Conference on Light Scattering of Solids*, edited by M. Bakanski (Flammarion, Paris, 1971), p. 483.

⁷C. W. Garland and D. D. Snyder, *J. Phys. Chem. Solids* **31**, 1759 (1970).

⁸C. W. Garland and R. Renard, *J. Chem. Phys.* **44**, 1130 (1966).

⁹C. K. Choo and C. W. Garland, *J. Chem. Phys.* **59**, 1541 (1973).

¹⁰According to C. H. Wang and R. B. Wright [*J. Chem. Phys.*]

- 57, 4401 (1972)], the tetragonal axis was aligned parallel to the direction of the temperature gradient in their Raman investigation. However, there is no evidence that this should always be true, and the present shear velocity data indicate that it is not.
- ¹⁰A. Bonilla, C. W. Garland, and N. E. Schumaker, *Acta Crystallogr. A* **26**, 156 (1970).
- ¹¹V. Hovi, K. Heiskanen, and M. Vartera, *Ann. Acad. Sci. Fenn. No. A144* (1964); V. Hovi, K. Paavola, and O. Urvas, *Ann. Acad. Sci. Fenn. No. A291* (1968).
- ¹²C. W. Garland and R. A. Young, *J. Chem. Phys.* **48**, 146 (1968).
- ¹³T. S. Velichkina, O. N. Golubeva, O. A. Shustin, and I. A. Yakovlev, *Bull. Acad. Sci. USSR Phys. Ser.* **35**, 932 (1971).
- ¹⁴K. Kawasaki, *Int. J. Magn.* **1**, 171 (1971).
- ¹⁵K. Kawasaki, *Phys. Rev. A* **1**, 1750 (1970).
- ¹⁶B. I. Halperin and P. C. Hohenberg, *Phys. Rev.* **177**, 952 (1969).
- ¹⁷G. E. Laramore and L. P. Kadanoff, *Phys. Rev.* **187**, 619 (1969).
- ¹⁸E. Riedel and F. Wegner, *Phys. Rev. Lett.* **24**, 730 (1970); E. K. Riedel, *J. Appl. Phys.* **42**, 1383 (1971).